Article

Base-by-Base Dynamics in DNA Hybridization Probed by Fluorescence Correlation Spectroscopy

Xudong Chen, Yan Zhou, Peng Qu, and Xin Sheng Zhao

J. Am. Chem. Soc., **2008**, 130 (50), 16947-16952 • DOI: 10.1021/ja804628x • Publication Date (Web): 19 November 2008

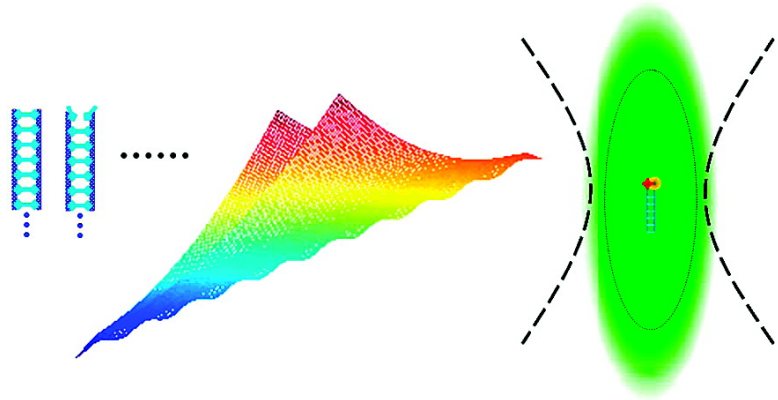

J|A|C|S
ARTICLES

Published on Web 11/19/2008

Base-by-Base Dynamics in DNA Hybridization Probed by Fluorescence Correlation Spectroscopy

Xudong Chen, Yan Zhou, Peng Qu, and Xin Sheng Zhao*

Beijing National Laboratory for Molecular Sciences, State Key Laboratory for Structural Chemistry of Unstable and Stable Species, and Department of Chemical Biology, College of Chemistry and Molecular Engineering, Peking University, Beijing 100871, China

Received June 17, 2008; E-mail: zhaoxs@pku.edu.cn

Abstract: Thermodynamics and dynamics of DNA hybridization/dehybridization at a terminal of a DNA duplex are investigated using steady-state fluorescence and fluorescence correlation spectroscopy (FCS). We introduce two pairs of dyes with different characteristic distances in fluorescence resonance energy transfer (FRET) to investigate the same process. The phenomenal discrepancy in the experimental observations between our two FRET pairs is incompatible with the traditional two-state model. We propose a so-called stretched exponential zipper (SEZ) model to successfully analyze the experimental data, through which the fundamental behavior of base-by-base hybridization/dehybridization is revealed. The dynamic parameters of the activation energy of single base-pair reaction derived from the two FRET pairs are consistent. The enthalpy change and entropy change of single base-pair formation are in agreement with theoretical prediction.

Introduction

DNA hybridization/dehybridization is a fundamental process in molecular biology and cell biology.[1] Although the kinetic and thermodynamic properties of short oligonucleotides and long DNAs have been investigated extensively, in recent years new techniques such as fluorescence correlation spectroscopy (FCS),[2−9] NMR,[10] and laser temperature jump[11,12] have been applied to understand the fast dynamics of DNA terminal-like structures.

FCS is a powerful tool to study the conformational fluctuations with a time resolution on the submicrosecond scale. The theory about FCS was established in the 1970s[13−16] and has been thoroughly reviewed (see, for example, ref 17). In principle, all processes that could induce fluorescence change are reflected in an FCS curve, which can be analyzed by dynamic differential equations. However, the ability of FCS to distinguish different processes on a similar time scale is limited by experimental errors. Therefore, the traditional fitting models were often simplified to two thermodynamic states or two radiation states.

Because of the ability to translate distance information to fluorescence intensity in real time, fluorescence resonance energy transfer (FRET) is often combined with FCS[2−9] to monitor the conformational changes in proteins and DNAs. Already, many researchers have investigated the terminal-like structure of the molecular beacon as a model system of DNA secondary structures using FCS and FRET, for the conversion between the open and closed states of hairpin proves to be an ideal case for such studies.[3−9] Although it is conceivable that DNA hybridization/dehybridization should proceed in a base-by-base manner, usually a two-state model is assumed when interpreting the experimental observations.[3,6−9] However, Van Orden's group[4,5] has found that it is necessary to improve the two-state model by considering a third state, and theoretical studies also suggest the existence of intermediate states in hairpin folding and unfolding.[18−21]

(1) Bloomfield, V. A.; Crothers, D. M., Tinoco, I. In *Nucleic Acids: Structure, Properties and Functions*; Stiefe, J., Ed.; University Science Books: Sausalito, CA, 2000; pp *1−10*, 598−724.
(2) Altan-Bonnet, G.; Libchaber, A.; Krichevsky, O. *Phys. Rev. Lett.* **2003**, *90*, 138101.
(3) Bonnet, G.; Krichevsky, O.; Libchaber, A. *Proc. Natl. Acad. Sci. U.S.A.* **1998**, *95*, 8602–8606.
(4) Jung, J.; Ihly, R.; Scott, E.; Yu, M.; Van Orden, A. *J. Phys. Chem. B* **2008**, *112*, 127–133.
(5) Jung, J.; Van Orden, A. *J. Am. Chem. Soc.* **2006**, *128*, 1240–1249.
(6) Kim, J.; Doose, S.; Neuweiler, H.; Sauer, M. *Nucleic Acids Res.* **2006**, *34*, 2516–2527.
(7) Wallace, M. I.; Ying, L.; Balasubramanian, S.; Klenerman, D. *J. Phys. Chem. B* **2000**, *104*, 11551–11555.
(8) Wallace, M. I.; Ying, L.; Balasubramanian, S.; Klenerman, D. *Proc. Natl. Acad. Sci. U.S.A.* **2001**, *98*, 5584–5589.
(9) Ying, L.; Wallace, M. I.; Klenerman, D. *Chem. Phys. Lett.* **2001**, *334*, 145–150.
(10) Wemmer, D. E.; Chou, S. H.; Hare, D. R.; Reid, B. R. *Nucleic Acids Res.* **1985**, *13*, 3755–3772.
(11) Ansari, A.; Kuznetsov, S. V. *J. Phys. Chem. B* **2005**, *109*, 12982–12989.
(12) Ansari, A.; Kuznetsov, S. V.; Shen, Y. *Proc. Natl. Acad. Sci. U.S.A.* **2001**, *98*, 7771–7776.
(13) Ehrenber, M.; Rigler, R. *Chem. Phys. Lett.* **1972**, *14*, 539–544.
(14) Ehrenber, M.; Rigler, R. *Chem. Phys.* **1974**, *4*, 390–401.
(15) Elson, E. L.; Magde, D. *Biopolymers* **1974**, *13*, 1–27.
(16) Magde, D.; Elson, E. L.; Webb, W. W. *Biopolymers* **1974**, *13*, 29–61.
(17) Krichevsky, O.; Bonnet, G. *Rep. Prog. Phys.* **2002**, *65*, 251–297.
(18) Bowman, G. R.; Huang, X.; Yao, Y.; Sun, J.; Carlsson, G.; Guibas, L. J.; Pande, V. S. *J. Am. Chem. Soc.* **2008**, *130*, 9676–9678.
(19) Errami, J.; Peyrard, M.; Theodorakopoulos, N. *Eur. Phys. J. E* **2007**, *23*, 397–411.
(20) Cuesta-Lopez, S.; Peyrard, M.; Graham, D. J. *Eur. Phys. J. E* **2005**, *16*, 235–246.
(21) Sorin, E. J.; Rhee, Y. M.; Nakatani, B. J.; Pande, V. S. *Biophys. J.* **2003**, *85*, 790–803.

Table 1. DNA Samples

index	sequence	modification	type
P	5′-tt cta gcc tga ctt ctt att-3′	3′-TMR	probe
Tp	5′-aat aag aag tca ggc tag aa-3′	none	target
Tpd	5′-aat aag aag tca ggc tag aa-3′	5′-Dabcyl	target
Tpf	5′-aat aag aag tca ggc tag aa-3′	5′-Cy5	target
Tn1	5′-tat aag aag tca ggc tag aa-3′	5′-Dabcyl	target
Tn2	5′-ttt aag aag tca ggc tag aa-3′	5′-Dabcyl	target
Tn3	5′-tta aag aag tca ggc tag aa-3′	5′-Dabcyl	target
Tn4	5′-tta tag aag tca ggc tag aa-3′	5′-Dabcyl	target
Tn5	5′-tta ttg aag tca ggc tag aa-3′	5′-Dabcyl	target

In previous work,[22−24] we have studied DNA hybridization/dehybridization on surfaces with electric potential and in solution between two single stranded DNAs (ssDNA) and a double stranded DNA (dsDNA). We found that the kinetic properties are different between structured and random coil DNAs.[22−24] It was also found that a zipper model is necessary for the experimental results and that the hairpin opening is in a concerted manner during the hybridization.[22]

In this article, we investigated the terminal behavior of a dsDNA through FRET and FCS by maintaining the temperatures far below the melting point of the duplex. Different from previous studies, two FRET pairs (carboxyltetramethylrhodamine (TMR)−indodicarbocyanine (Cy5) pair and TMR−Dabcyl pair) with different characteristic distances were introduced into a duplex to observe the same process for the purpose of obtaining base-by-base information. By monitoring the fluorescent signals, we measured the thermodynamic melting curves and FCS curves. The phenomenal discrepancy in the experimental observations between our two FRET pairs is incompatible with the traditional two-state model. Here we propose a new model, called a stretched exponential zipper (SEZ) model, to analyze our two independent sets of data simultaneously, in which several radiation states are considered according to the number of dissociated base pairs. The dynamic parameters of the activation energy of the single base-pair reaction derived from the two FRET pairs based on the SEZ model are consistent. The enthalpy change and entropy change of single base-pair formation are in agreement with theoretical prediction.[25] Enlightened by our results, we can have a better understanding on previous experimental observations.

Materials and Methods

Reagents. A 20-base oligonucleotide was chosen as a basic sequence (probe) and was labeled with carboxyltetramethylrhodamine (TMR) at the 3′ end, and other complimentary ssDNAs with different labeling were designed as targets for different purposes (Table 1). This piece of oligonucleotide is a fragment of the lipoprotein lipase gene. As is known, G base may quench fluorescence so that it can interfere with the experiment. Therefore, we chose A or T bases to connect the chromorphores. Otherwise, no other specialty was considered. The single base property studied in this paper is the average property without differentiating the nature of bases. All sequences were purchased from Sangon Company, China. Two classes of FRET pairs were designed: (a) donor TMR and quencher Dabcyl and (b) donor TMR and acceptor indodicarbocyanine (Cy5). Acceptors (Dabcyl and Cy5) were attached at the 5′ ends of targets. The structures and connection to DNA of the chromophores are shown in Figure 1.

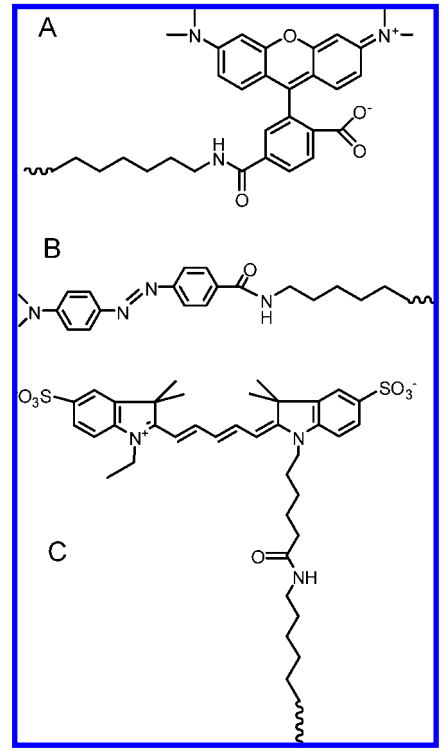

Figure 1. Structures of three chromophores and their connections to DNA as provided by the company. The wave lines represent DNA sequences. (A) TMR, (B) Dabcyl, and (C) Cy5.

We designed two FRET pairs with different characteristic distances which are TMR-Cy5 pair and TMR-Dabcyl pair. TMR was labeled at the 3′ end of an ssDNA named as P in Table 1. Cy5 or Dabcyl was labeled at the 5′ end of complementary strands of the probe, named as Tpf or Tpd (Table 1), respectively. To obtain the characteristic distance expressed in the number of dissociated base pairs at the DNA terminal, the FRET efficiency was measured in a set of mismatched dsDNAs.

The buffer was 200 mM NaCl and 1 × TE diluted from 20 × TE, which was purchased from Molecular Probe. The composition of 20 × TE was 0.2 M Tris-HCl and 0.02 M EDTA, with pH = 7.5. Water (18.2 MΩ·cm) was treated through PALL.

All the dsDNA samples were prepared by mixing the ssDNAs of probe and respective target, heating to 90 °C for 2 min and slowly cooling down to room temperature. The concentrations of the probe were 1 nM in the melting curve and FCS experiments and 50 nM in the measurement of the FRET characteristic distance. The concentration of target was 10 times that of the probe to make all probe sequences hybridized. Solutions in experiments were mixed with 0.01% Tween-20 to prevent surface adhesion of DNA.[7,8]

Melting Curve Measurement. The melting curve was recorded as previously reported.[22] The fluorescence was collected on a Renishaw1000 microscopic spectrometer (Britain) with a 514 nm argon ion laser (Melles Griot, USA) and THMS600 temperature controller (Linkam, Britain). The temperature range was from 5 to 80 °C.

In the TMR−Dabcyl system, the melting curve was obtained by measuring the fluorescence of TMR. The curve was corrected

(22) Chen, C. L.; Wang, W. J.; Wang, Z.; Wei, F.; Zhao, X. S. *Nucleic Acids Res.* **2007**, *35*, 2875–2884.
(23) Wei, F.; Chen, C. L.; Zhai, L.; Zhang, N.; Zhao, X. S. *J. Am. Chem. Soc.* **2005**, *127*, 5306–5307.
(24) Wei, F.; Qu, P.; Zhai, L.; Chen, C. L.; Wang, H. F.; Zhao, X. S. *Langmuir* **2006**, *22*, 6280–6285.
(25) SantaLucia, J. *Proc. Natl. Acad. Sci. U.S.A.* **1998**, *95*, 1460–1465.

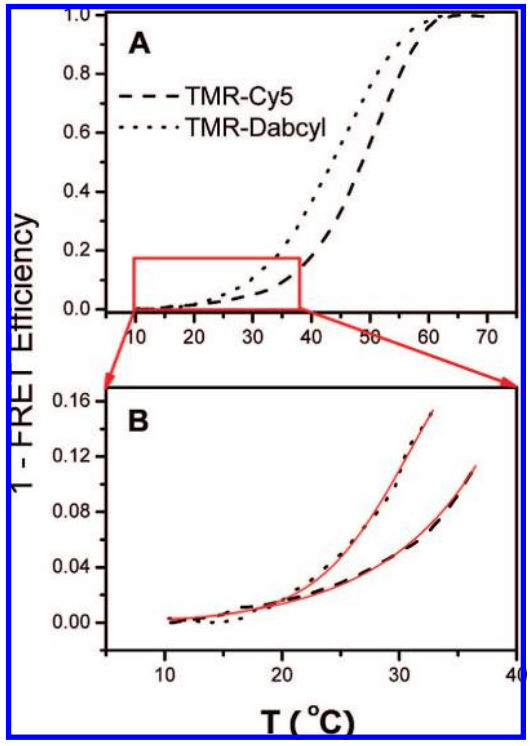

Figure 2. Experimental and simulated melting curves. (A) The whole experimental melting curves. (B) Part of A in a low temperature range together with the fitting by the zipper model. Dashed lines are experimental data, and solid lines are from the fitting.

by a control dsDNA (P and Tp) solely labeled by TMR, and the normalization FRET efficiency was calculated. In the TMR−Cy5 system, the fluorescence spectra of donor TMR and acceptor Cy5 were collected simultaneously, and assisted by the spectra of pure TMR and Cy5, the FRET efficiency was derived. Then, the melting curves were obtained by plotting FRET efficiency against temperature.

FCS Measurement. The FCS experiments were carried out on a homemade dual-channel fluorescence microscope[3,8] using a CW Ya-Ge laser (532 nm) (SUW Tech. China) excitation. The signal in the correct wavelength region was detected by two SPMDs (Perkin-Elmer AQR14) with appropriate filters placed in front of them. The fluctuation signals from the two channels were collected with a bin time of 6.4 μs by a correlator (www.correlator.com). The temperature in the FCS experiments was controlled by a THMS600 temperature controller (Linkam, Britain).

The fluorescence in the TMR−Dabcyl system was evenly split into two APD detectors, and an FCS curve was calculated by cross correlation of the signals from the two detectors. This was essentially a self-correlation, but instrumental noise could be greatly oppressed. The diffusion component in the FCS curve was removed through dividing the data by the FCS curve from the control experiments.[3] In the TMR−Cy5 system, the fluorescence between 670 and 735 nm was collected by one detector (A-channel) and that between 550 and 650 nm by another detector (B-channel). The ratio of A to a sum of A and B was calculated as FRET efficiency. The FCS curve was calculated from the ratio. With this method, the diffusion component was automatically removed.[7−9]

Results

Analysis of Melting Curves. Figure 2 shows the melting curves of dsDNAs composed of TMR−Dabcyl and TMR−Cy5,

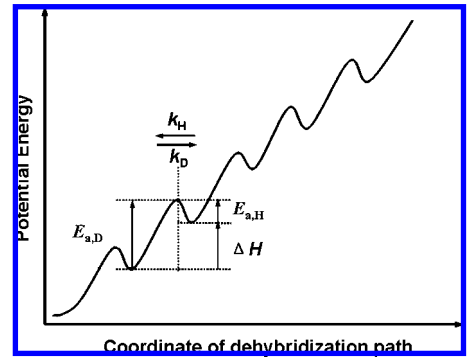

Figure 3. Sketch of energy profile along the dehybridization path at a dsDNA terminal. Thermodynamic and dynamic parameters for one base-pair reaction are illustrated.

and their melting temperatures differ by ~5 °C. Marrison and Stols,[26] Moreira et al.,[27] and our group[22] have investigated the thermodynamic effects of dye modification, and it is shown that the variation in the melting temperature is usually less than 1.5 °C. Therefore, the difference seen in Figure 2A should be carefully analyzed, which indicates that merely using a two-state model will not be able to account for our observation.

The zipper model has been developed as an effective model since 1960s.[25,28−32] Chen et al.[22] also used this model to interpret their kinetic data. In this model, the hybridization proceeds through initial nucleation and subsequent base-pair extension. The objective of present research is the terminal fluctuation in a dsDNA. According to the zipper model, the initial steps of dehybridization should proceed through dissociation of base pairs in a base-by-base manner (Figure 3). Because of different characteristic distances in FRET between TMR−Dabcyl and TMR−Cy5 systems, the base-by-base dissociation is sensed differently. The TMR−Dabcyl system undergoes dissociation at an earlier stage than the TMR−Cy5 system, for the former has a shorter characteristic FRET distance, which is reflected in Figure 2.

We now use the zipper model to fit the melting curves in the temperature range much lower (>10 °C) than the melting temperature, where only the terminal dissociation is detected by the FRET pairs. In this temperature range, bulge formation is thermodynamically unfavorable, and we neglect its contribution. Under this assumption, the solution contains partially dissociated dsDNAs of different extent, all starting from the dissociation of the end base pair and proceeding base-by-base. We denote x_i as the molar fraction of the species with i dissociated bases from the end with labeled dyes, so that

$$\sum_{i=0} x_i = 1 \qquad (1)$$

The equilibrium constant K_i between the i and $i-1$ species is related to the enthalpy of single base dehybridization ΔH_i and entropy of single base dehybridization ΔS_i by

(26) Morrison, L. E.; Stols, L. M. *Biochemistry* **1993**, *32*, 3095–3104.
(27) Moreira, B. G.; You, Y.; Behlke, M. A.; Owczarzy, R. *Biochem. Bioph. Res. Co.* **2005**, *327*, 473–484.
(28) Bommarito, S.; Peyret, N.; SantaLucia, J., Jr *Nucleic Acids Res.* **2000**, *28*, 1929–1934.
(29) Craig, M. E.; Crothers, D. M.; Doty, P. *J. Mol. Biol.* **1971**, *62*, 383–392.
(30) Porschke, D.; Uhlenbeck, O. C.; Martin FH, *Biopolymers* **1973**, *12*, 1313–1335.
(31) Wetmur, J. G.; Davidson, N. *J. Mol. Biol.* **1968**, *31*, 349–370.
(32) Zuker, M. *Nucleic Acids Res.* **2003**, *31*, 3406–3415.

$$\frac{x_i}{x_{i-1}} = K_i = \exp\left(-\frac{\Delta H_i - T\Delta S_i}{RT}\right) \quad (2)$$

where R denotes thermodynamic constant.

To simplify our data analysis, we assume that ΔH_i and ΔS_i are the same[25] and replace them by ΔH and ΔS:

$$\frac{x_i}{x_{i-1}} = K = \exp\left(-\frac{\Delta H - T\Delta S}{RT}\right) \quad (3)$$

From eq 3 we obtain

$$x_i = x_0 K^i \quad (4)$$

The FRET efficiency in species i is

$$E_i = \frac{R_C^6}{R_i^6 + R_C^6} \quad (5)$$

where R_i is the average distance between terminal chromophores in species i and R_C is the characteristic distance of FRET. The contribution of species i to the signal in the melting curve is

$$I_i \propto x_i(1 - E_i) = x_0 K^i \frac{R_i^6}{R_i^6 + R_C^6} \quad (6)$$

Further, we assume that the effective distance is linear to the number of dissociated bases, which should be acceptable when the number is not large.[33] By rewriting eq 6, the melting curve is predicted by

$$I = \sum_i I_i, \quad I_i \propto x_0 K^i \frac{(i + i_0)^6}{(i + i_0)^6 + i_C^6} \quad (7)$$

where i_0 represents the distance between the FRET pair when $i = 0$, and i_C is the characteristic distance expressed in the number of dissociated bases.

We recorded the melting curves of series of partially mismatched dsDNAs composed of P with Tpd, Tn1, Tn2, Tn3, Tn4, and Tn5, respectively (Table 1). By assuming that the effective distances of FRET pairs are identical between the dissociated P−Tpd duplex and respective mismatched duplexes in full hybridization, the fluorescence intensity at full hybridization obtained in Figure 4A is plotted against the number of mismatched bases to estimate i_C (Figure 4B). From the fitting, $i_0 = 1.0 \pm 0.1$ and $i_C = 3.3 \pm 0.2$ for the TMR−Dabcyl system are obtained. Knowing that R_C for the TMR−Dabcyl pair is 26 Å[34] and that for the TMR−Cy5 pair is 52 Å,[35] $i_C = 6.6 \pm 0.5$ for the TMR−Cy5 system is derived. Obviously, the assumption that connecting distance and the number of dissociated bases will be invalid when the number is large;[33] our treatment can only be applied in the temperature range far below the melting temperature. Here as in previous investigation, we assume that the FRET efficiency does not vary with temperature, which seems acceptable in a temperature range that is not large since the data are fitted reasonably well.

With all necessary information available, now we can fit the low temperature part of the melting curves by taking ΔH and ΔS as fitting parameters. In the fitting, the maximum number of dissociation bases needed is less than 8, because the concentration of larger dissociated species is negligible. We are happy to see that not only the melting curves are satisfactorily fit (Figure 2B) but also the two largely different melting curves result in identical thermodynamic parameters within the experimental error: $\Delta H = 8.5 \pm 1.2$ kcal mol^{-1} and $\Delta S = 23 \pm 3.2$ cal mol^{-1} K^{-1} from TMR−Dabcyl; $\Delta H = 8.0 \pm 1.8$ kcal mol^{-1} and $\Delta S = 26 \pm 6.0$ cal mol^{-1} K^{-1} from TMR−Cy5. ΔH and ΔS can also be estimated by web-available programs. A calculation for our system based on www.bioinfo.rpi.edu/applications/hybrid delivers the averaged values as $\Delta H = 8.0 \pm 0.1$ kcal mol^{-1} and $\Delta S = 22 \pm 0.2$ cal mol^{-1} K^{-1}, in agreement with our experimental results.

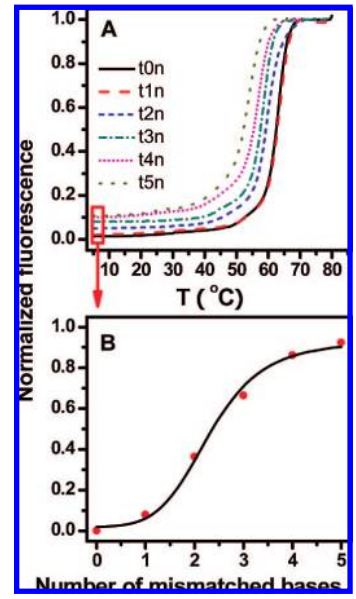

Figure 4. Derivation of the characteristic distance expressed in number of dissociated bases for the TMR-Dabcyl system. (A) The melting curves of a series of terminal mismatched dsDNAs. (B) Plot of fully hybridized fluorescence intensity vs number of mismatched bases and the fit of the FRET efficiency using eq 7.

Analysis on FCS Data. Some typical FCS data are shown in Figure 5. Although the two-state model has been widely used in previous FCS studies,[3,6−9] we have found its invalidation here. In fact, Jung and Van Orden [4,5] have already pointed out the limitation of the two-state model even in the fluctuation of hairpin structure.

We then carry out analysis of FCS data based on the zipper model similarly to our previous treatment on the melting curves. We denote k_H and k_D as the rate constants of single base-pair formation and dissociation, respectively (Figure 3), and C_i as the concentration of species i. The rate equation reads

$$\frac{dC_i}{dt} = k_D C_{i-1} - (k_D + k_H)C_i + k_H C_{i+1}, \quad \frac{k_D}{k_H} = K \quad (8)$$

Correspondingly, the dynamic matrix connecting all the species together[15,17] reads

$$M = \begin{vmatrix} -k_D & k_H & 0 & 0 & \cdots \\ k_D & -(k_D + k_H) & k_H & 0 & \cdots \\ 0 & k_D & -(k_D + k_H) & k_H & \cdots \\ \vdots & \vdots & \vdots & \vdots & \ddots \end{vmatrix} \quad (9)$$

Combining the matrix of eq 9 and the contribution of species i in eq 6, the FCS function, $G(\tau)$, is obtained as

(33) Yakushevich, L. V. In *Nonlinear Physics of DNA*; Holden, A. V., Ed.; Wiley-VCH Verlag-GmbH &Co. KGaA: Weinheim; Starauss GmbH: Morlenbach, 2004; pp 19−39.
(34) Bernacchi, S.; Mely, Y. *Nucleic Acids Res.* **2001**, *29*, e62.
(35) Dietrich, A.; Buschmann, V.; Muller, C.; Sauer, M. *Rev. Mol. Biotechnol.* **2002**, *82*, 211–231.

$$G(\tau) \propto \sum_{j,l} I_j I_l \langle \delta C_j(0)\, \delta C_i(\tau) \rangle \tag{10}$$

where τ is the lag time in the correlation function and δ stands for variational concentration. Taking the thermodynamic parameters (ΔH and ΔS) and characteristic distance (i_C) obtained in the melting curve study and introducing one rate constant (k_H or k_D) as a fitting parameter, the simulated FCS is obtained. Unfortunately, the simulation based on the simple zipper model does not consistently fit all the experimental FCS, and one example is shown in Figure 5A.

The contribution of every elementary process to the FCS curve in the simple zipper model is in one exponential form.[15,17] Previous researchers have proposed a stretched-exponential form[5−9] to improve two-state models in the analysis of FCS data. Physically, the stretched-exponential form describes the reactions with static disorder,[36−38] resulting in statistical distribution of reaction rates different from that of one exponential form. Kim et al.[6] show that the relaxation of one base pair follows the stretched-exponential form. Therefore, we adopt the stretched-exponential form into the zipper model and name our treatment as the stretched exponential zipper (SEZ) model.

In a static disordered system, the rate of a process is stochastic. The effective time-dependent rate, $k_{\text{eff}}(t)$, is related to a stretched parameter β and a reaction frequency ω as[37,38]

$$G(\tau) \propto \exp\left[\int_0^\tau k_{\text{eff}}(t)\, \mathrm{d}t\right] = \exp[-(\omega\tau)^\beta] \tag{11}$$

Now, the reaction rates of hybridization and dehybridization in one base pair are $k_{\text{H,eff}}(t)$ and $k_{\text{D,eff}}(t)$, and eq 8 should be modified to

$$\begin{cases} \dfrac{dC_i}{dt} = k_{\text{D,eff}}(t)C_{i-1} - (k_{\text{D,eff}}(t) + k_{\text{H,eff}}(t))C_i + k_{\text{H,eff}}(t)C_{i+1} \\ \dfrac{k_{\text{D,eff}}(t)}{k_{\text{H,eff}}(t)} = K = \exp\left(-\dfrac{\Delta H - T\Delta S}{RT}\right) \\ k_{\text{eff}}(t) = k_{\text{H,eff}}(t) + k_{\text{D,eff}}(t) \end{cases} \tag{12}$$

Accordingly, the dynamic matrix becomes time-dependent and reads

$$\mathrm{M}_{\text{SEZ}}(t) = \begin{vmatrix} -k_{\text{D,eff}}(t) & k_{\text{H,eff}}(t) & 0 & 0 & \cdots \\ k_{\text{D,eff}}(t) & -(k_{\text{D,eff}}(t) + k_{\text{H,eff}}(t)) & k_{\text{H,eff}}(t) & 0 & \cdots \\ 0 & k_{\text{D,eff}}(t) & -(k_{\text{D,eff}}(t) + k_{\text{H,eff}}(t)) & k_{\text{H,eff}}(t) & \cdots \\ \vdots & \vdots & \vdots & \vdots & \ddots \end{vmatrix} \tag{13}$$

where

$$\begin{cases} k_{\text{H,eff}}(t) = \dfrac{1}{1+K}\beta\omega^\beta t^{\beta-1} \\ k_{\text{D,eff}}(t) = \dfrac{K}{1+K}\beta\omega^\beta t^{\beta-1} \end{cases} \tag{14}$$

By taking variable transformation from t to $t' = t^\beta$, M_{SEZ} matrix is converted to a time-independent form (eq 15).

Then, the FCS curve can be calculated as before, using β and ω as fitting parameters. The calculated FCS curves match the experimental results at all temperatures for both TMR−Dabcyl and TMR−Cy5 systems well, and one example is given in Figure 5A. The average relaxation time $\langle\tau\rangle$ can be derived according to eq 16.[5−9]

$$\mathrm{M}_{\text{SEZ}} = \begin{vmatrix} -k'_{\text{D}} & k'_{\text{H}} & 0 & 0 & \cdots \\ k'_{\text{D}} & -(k'_{\text{D}} + k'_{\text{H}}) & k'_{\text{H}} & 0 & \cdots \\ 0 & k'_{\text{D}} & -(k'_{\text{D}} + k'_{\text{H}}) & k'_{\text{H}} & \cdots \\ \vdots & \vdots & \vdots & \vdots & \ddots \end{vmatrix}$$

$$k'_{\text{H}} = \frac{1}{1+K}\omega^\beta$$

$$k'_{\text{D}} = \frac{K}{1+K}\omega^\beta \tag{15}$$

$$\langle\tau\rangle = \int_0^\infty \exp[-(\omega t)^\beta]\, \mathrm{d}t = \frac{1}{\omega\beta}\Gamma\left(\frac{1}{\beta}\right),\ \Gamma(x) = \int_0^\infty t^{x-1}e^x\, \mathrm{d}t \tag{16}$$

Subsequently, the average rate constants of single base-pair reaction are obtained:

$$\begin{cases} \langle k_{\text{H}} \rangle = \langle k_{\text{H,eff}}(t) \rangle = \dfrac{1}{1+K} \cdot \dfrac{\omega\beta}{\Gamma(\beta^{-1})} \\ \langle k_{\text{D}} \rangle = \langle k_{\text{D,eff}}(t) \rangle = \dfrac{K}{1+K} \cdot \dfrac{\omega\beta}{\Gamma(\beta^{-1})} \end{cases} \tag{17}$$

The two sets of enthalpy and entropy of one base-pair reaction, ΔH and ΔS, obtained from the experimental melting curves of TMR−Cy5 and TMR−Dabcyl systems are used separately for the respective fit of the FCS data. The Arrhenius plots of $\langle k_{\text{H}} \rangle$ and $\langle k_{\text{D}} \rangle$from the SEZ model appear as good straight lines (Figure 6), from which the activation energy ($E_{\text{a,H}}$ and $E_{\text{a,D}}$) and the pre-exponential factor (A_{H} and A_{D}) of a single base reaction according to the equation

$$\langle k_{\text{H}} \rangle = A_{\text{H}} \exp\left(-\frac{E_{\text{a,H}}}{RT}\right),\ \langle k_{\text{D}} \rangle = A_{\text{D}} \exp\left(-\frac{E_{\text{a,D}}}{RT}\right) \tag{18}$$

are derived, and they are presented in Table 2. Again, to our satisfaction, not only all FCS data can be well fit with the SEZ model, but also the largely different behaviors of the two labeling pairs result in consistent dynamic parameters within the experimental error (Table 2).

Discussion

Theoretically, DNA dehybridization can occur in much more complicated ways. For example, dissociation could start from any place in a dsDNA, and bulges of different sizes could form during the process. To simplify the treatment, in our SEZ model we only consider the base-by-base reaction starting from the first base at the end labeled with dyes. It is reasonable to assume that the bulge formation needs more energy than base-by-base dissociation, so that the population of the species based on the bulge formation is low at the temperature range well below the melting temperature. DsDNA dehybridization can also start at places not sensitive to the dyes, e.g., the other end. As long as our focus is on the process noticed by the dyes, it does not matter what happens in other places in the dsDNA provided that the events do not affect our process. The melting curve at high temperature contains contribution from all factors. Therefore, our SEZ model is applicable only in a low temperature range where the most prominent registered process is the terminal fluctuation. The good and consistent fit demonstrates that our assumption is valid in the current situation.

(36) Klafter, J.; Shlesinger, M. F. *Proc. Natl. Acad. Sci. U.S.A.* **1986**, *83*, 848–851.
(37) Kou, S. C.; Xie, S.; Liu, J. S. *J. Roy. Stat. Soc. C-App.* **2005**, *54*, 469–506.

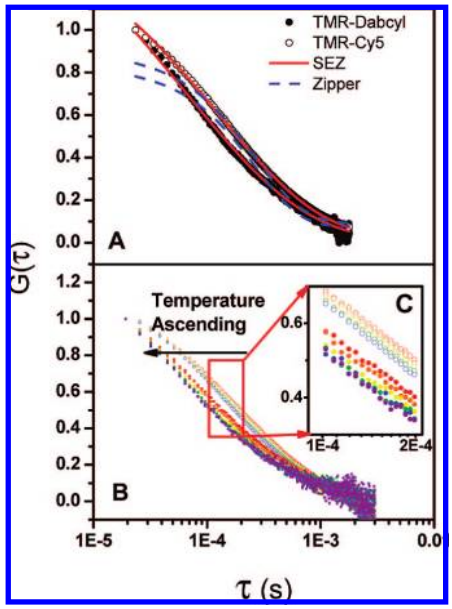

Figure 5. Experimental and simulated FCS curves. (A) Experimental FCS data and their fitting by zipper model and SEZ model, respectively, at 26.4 °C for TMR−Dabcyl system and 27.3 °C for TMR−Cy5 system. (B) Series of experimental FCS curves of TMR−Dabcyl and TMR−Cy5 systems at different temperatures. Inset shows the expanded view. Open circles are for TMR−Cy5, and solid circles for TMR−Dabcyl.

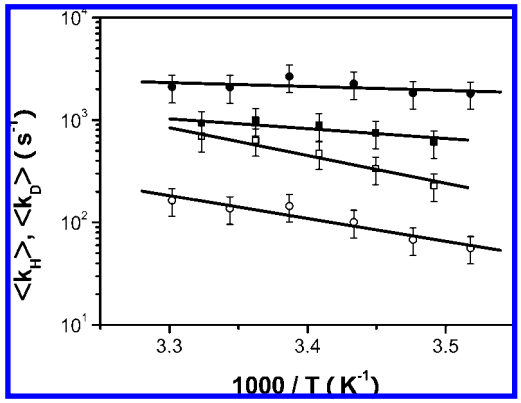

Figure 6. Arrhenius plots of averaged rate constants from the SEZ model. Squares are for the TMR−Cy5 system, and circles are for the TMR−Dabcyl system. Hollow points are for $\langle k_D \rangle$, and solid points are for $\langle k_H \rangle$. From the linear fit, the activation energy and the pre-exponential factor can be derived, and the results are shown in Table 2.

Table 2. Activation Energies and Pre-Exponential Factors from the SEZ Model

	TMR−Cy5	TMR−Dabcyl
$E_{a,H}$ (kcal mol^{-1})	4.4 ± 1.0	1.7 ± 1.5
$\ln(A_H/s^{-1})$	16.0 ± 5.0	10.0 ± 5.2
$E_{a,D}$ (kcal mol^{-1})	12.4 ± 1.0	10.2 ± 1.5
$\ln(A_D/s^{-1})$	29.1 ± 5.0	22.2 ± 5.2

Using the SEZ model, different thermodynamic and dynamic behaviors of two pairs of dye labeling reach harmony on the basis of the same molecular properties. Especially, we have derived the activation energy of a single base-pair reaction. We see that the transition state of the reaction has a small energy barrier of a few kcal mol^{-1} even along the downhill hybridization direction. Pictorially, before the hydrogen bond formation, the approaching groups have to adjust their solvation environment and charge distribution, which likely creates a noticeable energy barrier. The introduction of a statistical distribution of the rate constant in a single base reaction reflected by the stretched-exponential form is reasonable. Although there is only one lowest reaction path in the profile of the potential energy surface, the configurational space of DNA is extremely complex. Under finite temperature, the system can populate the configurations in the vicinity of the lowest energy path statistically, so that the rate constant becomes statistically distributed.

Although DNA hybridization/dehybridization proceed in a base-by-base manner, usually a two-state model is assumed in FRET studies, especially in the structural fluctuation of the hairpin, where both Arrhenius and non-Arrhenius behaviors are observed.[3,6−9] Recently, Jung and Van Orden point out that the two-state model is insufficient to explain their results and propose the existence of a third state.[4,5] In the theoretical work on hairpin RNA by Pande and co-workers[18,21] not only the intermediate states are predicted, but also the neighborhood process is suggested as the main route of the hairpin folding and unfolding. Compared with previous work, two FRET pairs of different characteristic distances are combined to study the behavior of one dsDNA sequence by us for the first time. The more stringent test makes invalidation of the two-state model more prominent. Our results are consistent with the theoretical prediction.

It seems clear now why the two-state model can approximately account for most previous experimental observations. The characteristic distance of most dye pairs in the FRET study is comparable to that for TMR−Cy5. This work finds that the equivalent characteristic number of dissociated bases is 6.6 for TMR−Cy5. Therefore, the region of switching from high FRET efficiency to low FRET efficiency is not sensed by a short hairpin stem; i.e., the hairpin's opening and closing can be viewed as a two-state process as far as the FRET efficiency is concerned. If one uses an FRET pair of short characteristic distance or in a longer hairpin stem, the base-by-base reaction will map through the sensitive variation region of FRET efficiency, and the two-state model will disclose its defect.

Conclusion

Using an FCS technique, two pairs of FRET dyes with different characteristic distances are introduced in one dsDNA to investigate its terminal fluctuation. A traditional two-state model is found invalid in the interpretation of our experimental observations. We have proposed the SEZ model, an extension of the zipper model, to successfully fit all experimental data in a consistent manner. Both thermodynamic and dynamic parameters for a single base-pair reaction are obtained, which provides base-by-base information on DNA hybridization/dehybridization. The SEZ model can shine some light on the understanding of previous experimental results.

Acknowledgment. This work was supported by NKBRSF (2006CB910304) and by NSFC (20673002 and 20733001).

Note Added after ASAP Publication. This article was published on the Web with minor errors in eqs 4, 6, 7 and text following eq 7. The correct version posted December 10, 2008 and the print version are correct.

JA804628X

(38) Vlad, M. O.; Ross, J.; Huber, D. L. *J. Phys. Chem. B* **1999**, *103*, 1563–1580.